

# Raman spectroscopy evidence of domain walls in the organic electronic ferroelectrics (TMTTF)<sub>2</sub>X (X = SbF<sub>6</sub>, AsF<sub>6</sub>, PF<sub>6</sub>)

Roman Świetlik\* and Bolesław Barszcz

*Institute of Molecular Physics, Polish Academy of Sciences, ul. Mariana Smoluchowskiego 17, 60-179 Poznań, Poland*

Andrej Pustogow and Martin Dressel

*1. Physikalisches Institut, Universität Stuttgart, Pfaffenwaldring 57, D-70550 Stuttgart, Germany*

(Received 29 September 2016; revised manuscript received 3 January 2017; published 21 February 2017)

Charge ordering in the quasi-one-dimensional organic conductors (TMTTF)<sub>2</sub>X (X = SbF<sub>6</sub>, AsF<sub>6</sub>, PF<sub>6</sub>) was studied by using Raman spectroscopy. In the charge-ordered phase three vibrational features related to the ring breathing mode  $\nu_{10}(a_g)$  of neutral (TMTTF<sup>0</sup>) and ionized (TMTTF<sup>+0.5</sup> and TMTTF<sup>+1</sup>) are observed at about 503, 507, and 526 cm<sup>-1</sup>, respectively. The bands of donor molecules with charge +0.5e are assigned to ferroelectric domains while the bands of neutral and fully ionized molecules to domain walls. The shape of the band at about 526 cm<sup>-1</sup>, attributed to the charged domain walls (molecules with charge +1e), reveals important differences between salts, i.e., indicates the presence of relaxor ferroelectricity which is well seen in (TMTTF)<sub>2</sub>PF<sub>6</sub>.

DOI: [10.1103/PhysRevB.95.085205](https://doi.org/10.1103/PhysRevB.95.085205)

## I. INTRODUCTION

For many years the organic conductors (TMTTF)<sub>2</sub>X with octahedral (X = SbF<sub>6</sub>, AsF<sub>6</sub>, PF<sub>6</sub>) or tetrahedral (X = BF<sub>4</sub>, ReO<sub>4</sub>) anions attract considerable attention, mainly because at low temperatures they undergo charge ordering (CO) transitions which give rise to electronic ferroelectricity [1–4]. These compounds are considered as model strongly correlated quasi-one-dimensional systems in which the interplay between spin, charge, and lattice degrees of freedom plays a very important role. The CO transition is discussed as a cooperative effect being the consequence of long-range Coulomb repulsion and donor-acceptor interactions [5].

Here we focus on three isostructural (TMTTF)<sub>2</sub>X salts with centrosymmetric anions (X = SbF<sub>6</sub>, AsF<sub>6</sub>, PF<sub>6</sub>) which exhibit metallic-like properties at room temperature (RT) and transitions to the CO state at  $T_{CO} = 157$ , 102, and 67 K, respectively. On further cooling down they undergo either a spin-Peierls transition [at 13 K for (TMTTF)<sub>2</sub>AsF<sub>6</sub> and 19 K for (TMTTF)<sub>2</sub>PF<sub>6</sub> salts] or antiferromagnetic ordering [at 8 K for (TMTTF)<sub>2</sub>SbF<sub>6</sub> salt] [6]. At RT the salts crystallize in the centrosymmetric triclinic structure with two donor molecules and one acceptor in the unit cell [5]. The planar organic donors are arranged into weakly dimerized stacks along the *a* axis; the neighboring stacks weakly interact along the *b* axis and are separated by anions in the *c* direction. When the anion size increases (PF<sub>6</sub> → AsF<sub>6</sub> → SbF<sub>6</sub>) the unit cell grows and the salt becomes more one-dimensional as a consequence of decreasing interactions along the *b* and *c* direction; the increase of one-dimensionality influences the position in the pressure-temperature phase diagram [6]. The ferroelectric nature of the CO state in these salts was shown by dielectric measurements ((TMTTF)<sub>2</sub>PF<sub>6</sub> [7], (TMTTF)<sub>2</sub>AsF<sub>6</sub> [8], (TMTTF)<sub>2</sub>SbF<sub>6</sub> [9,10]). The analysis of the relaxation processes below and above  $T_{CO}$  in the (TMTTF)<sub>2</sub>AsF<sub>6</sub> salt provides arguments for the existence of charged domain walls separating domains of opposite polarization [11–13]; the

charged domain walls were considered as charged solitons [3]. The ferroelectric domains on the nanometer scale were also shown by the observation of the crystal mosaic structure in the vicinity of CO [14]. Nevertheless no hysteresis loop could be observed because of the relatively high conductivity, i.e., high density of charge carriers which effectively screen the electric field. It is important that the dielectric constant, estimated from the values of dipole moments induced by CO on the TMTTF stacks, is smaller by a factor of ten in comparison with the large values of the dielectric constant measured around  $T_{CO}$  for (TMTTF)<sub>2</sub>AsF<sub>6</sub> [4]. This large discrepancy may be an indication that the domain walls rather than the dipoles inside domains mainly contribute to the large dielectric constant. Moreover, it should be also noted that the dielectric constant in the vicinity of CO is strongly sample dependent and even specimens of the same salt can exhibit different degrees of disorder when prepared in different electrocrystallization processes [2,4,7].

It is well known that infrared (IR) and Raman spectroscopies are very good experimental tools for investigating the charge residing on molecules in conducting stacks and thus its changes due to the CO transitions. Most charge sensitive are vibrational modes of TMTTF related to the stretching of C = C bonds, therefore they were mostly used for studies of the CO. There are two totally symmetric C = C modes  $\nu_3(a_g)$  and  $\nu_4(a_g)$ , and one asymmetric mode  $\nu_{28}(b_{1u})$  which are observed at 1639, 1538, and 1627 cm<sup>-1</sup> for neutral TMTTF<sup>0</sup>, respectively. When the ionization degree of the molecule grows these modes shift linearly towards lower wave numbers, and for the fully ionized TMTTF<sup>+</sup> the shift equals to 72, 120, and 80 cm<sup>-1</sup>, respectively [15,16]. For evaluating the charge distribution in conducting TMTTF stacks the IR active  $\nu_{28}(b_{1u})$  mode is most useful since it does not couple with the electronic background. The charge density can be also estimated using the position of the  $\nu_3(a_g)$  band, however the  $\nu_4(a_g)$  mode is not useful because of strong interaction with electrons. The IR and Raman studies of charge ordering in (TMTTF)<sub>2</sub>X (X = SbF<sub>6</sub>, AsF<sub>6</sub>, PF<sub>6</sub>) were reported and summarized in Refs. [16–19]. Other charge sensitive modes, which could be used for the charge density estimation, are the

\*swietlik@ifmpan.poznan.pl

C-S stretching ring breathing modes  $\nu_{10}(a_g) = 494 \text{ cm}^{-1}$  and  $\nu_{35}(b_{1u}) = 439 \text{ cm}^{-1}$  for  $\text{TMTTF}^0$ , but up to date they were basically not studied. Due to ionization the positions of these modes shift towards higher wave numbers, reaching the value  $29 \text{ cm}^{-1}$  for the fully ionized  $\text{TMTTF}^+$  [15,16]. Although the shift is considerably smaller in comparison with the C = C modes, it is sufficiently large for proper estimation of the ionization degree of TMTTF donors. In this paper we show that Raman bands assigned to these modes can be not only used as a sensitive indicator of the charge redistribution in TMTTF stacks but they also provide new information about the ferroelectric CO phase. The Raman  $\nu_{10}(a_g)$  bands are easy to observe when the spectrum is excited by the red laser (632.8 nm) due to significant intensity enhancement by resonance Raman effect; this effect also enhances the intensity of the C = C bands [15]. Namely, the  $(\text{TMTTF})_2^+$  dimers have a strong electronic absorption centered at about 667 nm and polarized perpendicularly to the TMTTF stacks [20].

## II. EXPERIMENT

Single crystals of the salts  $(\text{TMTTF})_2X$  ( $X = \text{SbF}_6, \text{AsF}_6, \text{PF}_6$ ) were grown by the standard electrochemical method. Raman spectra were measured in a backscattering geometry on a Horiba Jobin Yvon Labram HR 800 spectrometer equipped with a He-Ne laser ( $\lambda = 632.8 \text{ nm}$ ) and a liquid-nitrogen cooled CCD detector; for calibration the Si line at  $520.7 \text{ cm}^{-1}$  was used. The spectra were recorded for the electrical vector of the incident beam polarized perpendicular to the stacking  $a$  axis to profit of resonance effects, but the polarization of scattered radiation was not studied. The laser beam was focused on the best developed (001) crystal face; the diameter of the irradiation area was several micrometers (typically  $4 \mu\text{m}$ ). It is very important that the laser beam does not influence the sample, i.e., its power is low enough. For this reason, some preliminary investigations of the spectra as a function of the laser power were done. Though for our experimental setup the power of about 0.1 mW was found as very suitable, it was reduced down to about 0.04 mW. A typical time of a single spectrum accumulation was about 40 s and the spectrum at a given temperature was determined after averaging over about 30 accumulations.

For low-temperature investigations, the samples were placed in a continuous flow helium microscope cryostat (Oxford Instruments CF2102) with quartz windows. The single crystals were mounted on the cryostat cold finger by using vacuum grease. The spectra were studied in the temperature range  $T = 10\text{--}290 \text{ K}$ . Typical temperature variation rate was about 1 K/min.

## III. RESULTS AND DISCUSSION

Room temperature Raman spectra of the  $(\text{TMTTF})_2\text{AsF}_6$  and  $(\text{TMTTF})_2\text{PF}_6$  salts, measured for our samples with the excitation  $\lambda = 632.8 \text{ nm}$ , are very similar to those obtained with the excitation  $\lambda = 647.2 \text{ nm}$  [16]. Additionally, we have recorded the spectra of the  $(\text{TMTTF})_2\text{SbF}_6$  salt which are also very similar.

The temperature dependence of the Raman spectra of the  $(\text{TMTTF})_2\text{AsF}_6$  salt in the region of C = C stretching

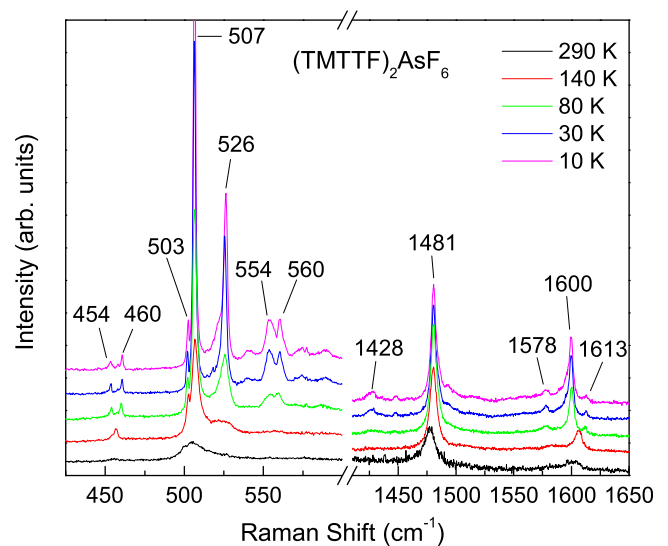


FIG. 1. Raman spectra of  $(\text{TMTTF})_2\text{AsF}_6$  salt obtained for the electrical vector of the exciting beam polarized perpendicular to the stacking axis for the red excitation  $\lambda = 632.8 \text{ nm}$ .

modes ( $1400\text{--}1650 \text{ cm}^{-1}$ ) and ring breathing modes ( $400\text{--}600 \text{ cm}^{-1}$ ) is shown in Fig. 1. At  $T = 290 \text{ K}$  we observe the following strong bands assigned to the totally symmetric  $a_g$  modes:  $\nu_3(a_g) = 1603 \text{ cm}^{-1}$ ,  $\nu_4(a_g) = 1477 \text{ cm}^{-1}$ , and  $\nu_{10}(a_g) = 505 \text{ cm}^{-1}$  with a shoulder at about  $500 \text{ cm}^{-1}$ . Taking into account the stack dimerization these bands can be related to in-phase  $a_g$  vibrations of molecules in a dimer (dimeric mode). Additionally, in the spectrum one can see a shoulder at  $1580 \text{ cm}^{-1}$ , which was assigned to the Raman active antiphase combination of the  $\nu_{28}(b_{1u})$  mode in TMTTF dimers [16]. In the region of the ring breathing modes we see also a weak band at  $457 \text{ cm}^{-1}$ , analogously assigned to the antiphase combination of the  $\nu_{35}(b_{1u})$  mode. On temperature decreasing down to  $T_{\text{CO}} = 102 \text{ K}$  all the  $a_g$  modes in the  $(\text{TMTTF})_2\text{AsF}_6$  salt slightly shift towards higher wave numbers but their positions correspond quite well to the average charge density  $+0.5e$  on the donor molecule. Below  $T_{\text{CO}}$ , the  $\nu_3(a_g)$  band splits into two components giving thus an evidence of the CO transition. At about 10 K the wave numbers of the  $\nu_3(a_g)$  split bands are  $1600$  and  $1613 \text{ cm}^{-1}$ , and are nearly the same as those reported previously for excitation  $647.2 \text{ nm}$  in Ref. [16], nevertheless, there exist also small differences. In our experiments just below  $T_{\text{CO}}$  the intensity of the lower-energy component was much higher than the higher-energy one, whereas in Ref. [16] they were comparable. Moreover, the temperature dependence of the intensity of the higher-energy  $\nu_3(a_g)$  component is also slightly different. Most probably these differences are due to various degrees of disorder in our crystals. The splitting is not seen for the  $\nu_4(a_g)$  mode because of the strong coupling with the electronic system (the coupling constants:  $g(\nu_3) = 0.03 \text{ eV}$  and  $g(\nu_4) = 0.12 \text{ eV}$  [21]). As shown by Yamamoto and Yakushi [22], for radical cation dimers with large electron-molecular vibration (EMV) coupling constants, the frequency of the Raman active in-phase dimeric mode is nearly independent on the charge distribution among the molecules in dimer and it corresponds to the average charge residing on the dimer. More interesting spectral changes

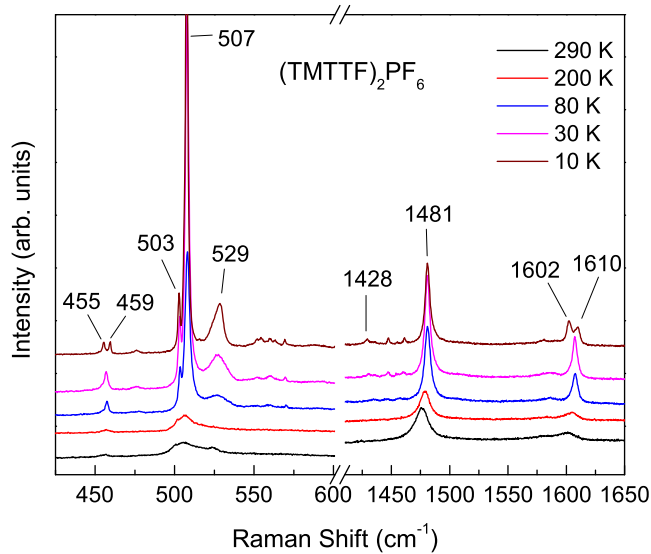


FIG. 2. Raman spectra of  $(\text{TMTTF})_2\text{PF}_6$  salt obtained for the electrical vector of the exciting beam polarized perpendicular to the stacking axis for red excitation  $\lambda = 632.8$  nm.

are observed in the lower wave number region of the ring breathing modes of the TMTTF molecule. On temperature decreasing the  $\nu_{10}(a_g)$  band slightly shifts towards higher wave numbers (reaching about  $507\text{ cm}^{-1}$  at 10 K) and its intensity strongly grows but without any visible modifications due to CO, as observed for the modes with strong EMV coupling ( $g(\nu_{10}) = 0.06\text{ eV}$  [21]), similarly as for the  $\nu_4(a_g)$  mode. The most important spectral change is that below  $T_{\text{CO}}$  a new band at about  $526\text{ cm}^{-1}$  appears whose intensity strongly increases on further cooling down. Taking into account its position it can be attributed to the  $\nu_{10}(a_g)$  mode of  $\text{TMTTF}^+$  ions (fully ionized molecules). Additionally, above  $T_{\text{CO}}$  a shoulder centered at about  $523\text{ cm}^{-1}$  is well seen which we relate to pretransitional charge fluctuations. Simultaneously, below  $T_{\text{CO}}$  we observe a much weaker and narrower band at  $502\text{ cm}^{-1}$  related to neutral  $\text{TMTTF}^0$  molecules. Additionally, we see that below  $T_{\text{CO}}$  the  $\nu_{35}(b_{1u})$  mode splits into two lines at about  $454$  and  $460\text{ cm}^{-1}$  providing the next clear evidence of the charge ordering, in agreement with the spectral behavior in the C = C stretching region. Below  $T_{\text{CO}}$  we also see a doublet at  $554$  and  $560\text{ cm}^{-1}$  which we assign to the  $\nu_9(a_g)$  mode of charge poor and charge rich molecules, respectively.

Both above and below  $T_{\text{CO}}$  the Raman spectra of  $(\text{TMTTF})_2\text{PF}_6$  (Fig. 2) and  $(\text{TMTTF})_2\text{SbF}_6$  (Fig. 3) are similar and exhibit analogous temperature behavior as observed for  $(\text{TMTTF})_2\text{AsF}_6$ . The three spectral features attributed to the ring breathing  $\nu_{10}(a_g)$  mode we interpret in the similar way, i.e., as a consequence of the presence of neutral and fully ionized molecules. However, a difference in comparison with the Raman spectra for the  $(\text{TMTTF})_2\text{PF}_6$  salt in Ref. [16] have been found, namely, for the  $\nu_3(a_g)$  mode we did not observe splitting just below  $T_{\text{CO}}$  but at lower temperature. Simultaneously, the same behavior was found for the  $\nu_{35}(b_{1u})$  mode. This difference can be related to larger sensitivity of the  $(\text{TMTTF})_2\text{PF}_6$  salt for defects in comparison with the other two salts. A difference between these salts was also found

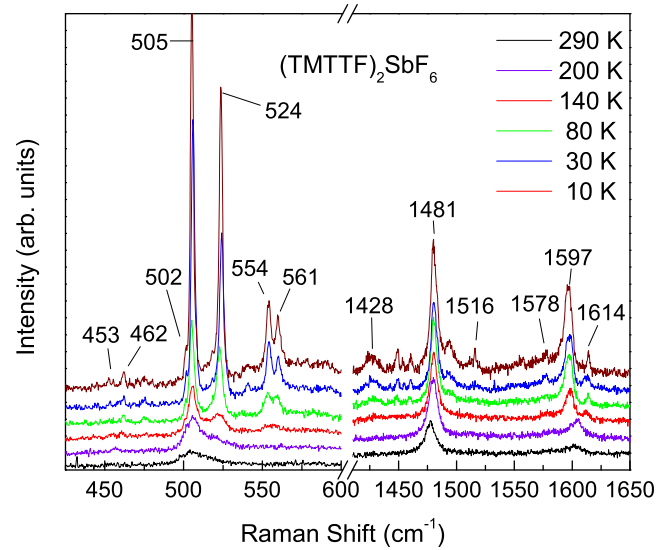


FIG. 3. Raman spectra of  $(\text{TMTTF})_2\text{SbF}_6$  salt obtained for the electrical vector of the exciting beam polarized perpendicular to the stacking axis for red excitation  $\lambda = 632.8$  nm.

in the dielectric measurements:  $(\text{TMTTF})_2\text{PF}_6$  shows relaxor ferroelectricity [7]. On the other hand, it is to be mentioned that the Raman spectra of the  $(\text{TMTTF})_2\text{PF}_6$  salt presented in Ref. [16] also do not exhibit visible modifications at  $T_{\text{CO}}$  but at slightly lower temperature.

The most important vibrational features for the three studied salts, together with their precise wave numbers, are listed in Table I. Taking into account the positions of split bands related to the  $\nu_3(a_g)$  mode and the  $\nu_{35}(b_{1u})$  mode we have calculated the charge density difference between charge rich and charge poor molecules  $2\delta$ . The obtained results for the  $\nu_3(a_g)$  mode are close to those determined from previous Raman measurements:  $2\delta(\text{AsF}_6) = 0.21e$  and  $2\delta(\text{PF}_6) = 0.12e$  at about 10 K [16]. However, the parameters  $2\delta$  estimated from the splitting of the  $\nu_{35}(b_{1u})$  mode at 10 K are larger (see Table I) but close to the values estimated from IR spectra on the basis of the  $\nu_{28}(b_{1u})$  C = C stretching mode, i.e.,  $0.29e(\text{SbF}_6)$ ,  $0.21e(\text{AsF}_6)$ , and  $0.15e(\text{PF}_6)$  [16]. Evidently, the  $b_{1u}$  modes are better indicators for estimation of the charge density also when observed as the antiphase dimeric mode in Raman spectra.

As already discussed above, the Raman  $\nu_{10}(a_g)$  features below  $T_{\text{CO}}$  at about  $503$ ,  $507$ , and  $526\text{ cm}^{-1}$  can be attributed to the neutral  $\text{TMTTF}^0$ , in-phase dimeric modes of  $(\text{TMTTF})_2^+$ , and fully ionized  $\text{TMTTF}^+$ , respectively (Fig. 4). We suggest that the strongest band at  $507\text{ cm}^{-1}$  is due to  $(\text{TMTTF})_2^+$  dimers in ferroelectric domains, while the bands  $502$  and  $523\text{ cm}^{-1}$  are due to neutral and charged domain walls which separate domains of opposite polarizations. The domain walls in electronic ferroelectrics  $(\text{TMTTF})_2X$  were considered as solitons [3]. The  $\nu_{10}(a_g)$  features are similar in the studied salts, however it exists also an important difference. Namely, when the size of the anion gets smaller, i.e., the anisotropy of these quasi-one-dimensional salts is reduced, the intensity of the  $\text{TMTTF}^+$  band at  $526\text{ cm}^{-1}$  decreases in comparison with the band at  $506\text{ cm}^{-1}$  and simultaneously a shoulder on

TABLE I. Main vibrational bands in Raman spectra of the salts  $(\text{TMTTF})_2X$  ( $X = \text{SbF}_6, \text{AsF}_6, \text{PF}_6$ ) for selected temperatures above and below the charge ordering transitions ( $2\delta$  is charge difference between molecules in dimer).

Mode	$(\text{TMTTF})_2\text{SbF}_6$ $T_{\text{CO}} = 157 \text{ K}$			$(\text{TMTTF})_2\text{AsF}_6$ $T_{\text{CO}} = 102 \text{ K}$			$(\text{TMTTF})_2\text{PF}_6$ $T_{\text{CO}} = 67 \text{ K}$		
	200 K	10 K	$2\delta$ at 10 K	140 K	10 K	$2\delta$ at 10 K	80 K	10 K	$2\delta$ at 10 K
$\nu_3(a_g)$	1604	1614 1597	0.24	1606	1613 1600	0.18	1606	1610 1602	0.11
$\nu_4(a_g)$	1480	1480.6		1480.4	1480.6		1481.0	1480.8	
$\nu_9(a_g)$	–	561 554		557	560.3 554.0		557	560 554	
$\nu_{10}(a_g)$	520	524.2		–	526.2		526.0	529.0	
	506	505.3		506.7	506.5		508.1	506.7	
$\nu_{35}(b_{1u})$	502	501.6		502.7	502.5		503.5	502.5	
	457	461.8 453.0	0.29	456.7	460.7 453.0	0.25	457.4	459.4 455.3	0.14

its low-energy side grows. This behavior can be correlated with differences between the salts observed in the dielectric data. As results from the temperature dependence of the dielectric constant, ferroelectric relaxors exist in  $(\text{TMTTF})_2\text{PF}_6$  [7]. A common feature of the ferroelectric relaxors is an existence of disorder which leads to a distribution of the Curie temperatures. Evidently the  $(\text{TMTTF})_2\text{PF}_6$  samples are less homogeneous (nanodomain size distribution) than those of  $(\text{TMTTF})_2\text{AsF}_6$  and  $(\text{TMTTF})_2\text{SbF}_6$  and this difference has an influence on the intensity and shape of the band at  $526 \text{ cm}^{-1}$ . The relaxor ferroelectric state was also suggested for the  $(\text{TMTTF})_2\text{AsF}_6$  salt [12]. Within our interpretation a shoulder at about  $520 \text{ cm}^{-1}$  [Fig. 4(b)], which grows on cooling down, can be considered as a signature of existence of relaxors in the  $(\text{TMTTF})_2\text{AsF}_6$  compound; an analogous shoulder is not observed for  $(\text{TMTTF})_2\text{SbF}_6$  [Fig. 4(a)]. If the charge order pattern of the type  $\dots +0+0+0+0+0+\dots$  (where  $+$  is charge rich and  $0$  is charge poor molecule) is assumed, one can imagine two types of domain walls

separating domains of different polarization in stacks, i.e., neutral (00) and charged (++) , which are related to the bands  $503$  and  $526 \text{ cm}^{-1}$ , respectively. If such domain walls exist, it seems that molecules inside these walls should interact rather weakly since no indication of charge-transfer transition between  $\text{TMTTF}^+$  ions was found in IR spectra of these salts [23]. It is also possible that the domain wall structure is more complicated and the bands  $503$  and  $526 \text{ cm}^{-1}$  are associated with single molecules. Our Raman data for  $(\text{TMTTF})_2\text{PF}_6$  [Fig. 4(c)] and partially also for  $(\text{TMTTF})_2\text{AsF}_6$  [Fig. 4(b)] seem to suggest that there exist various domain walls of slightly different properties. No doubt, this problem should be studied in more detail.

An important question is why the  $\text{TMTTF}^+$  ions and neutral  $\text{TMTTF}^0$  are only seen for Raman bands related to the  $\nu_{10}(a_g)$  mode and not for the  $\text{C}=\text{C}$  stretching  $\nu_3(a_g)$  and  $\nu_4(a_g)$  modes. At the moment the answer is not clear and further investigations are necessary. Evidently the  $\nu_{10}(a_g)$  mode is especially sensitive and yields Raman bands of large intensity

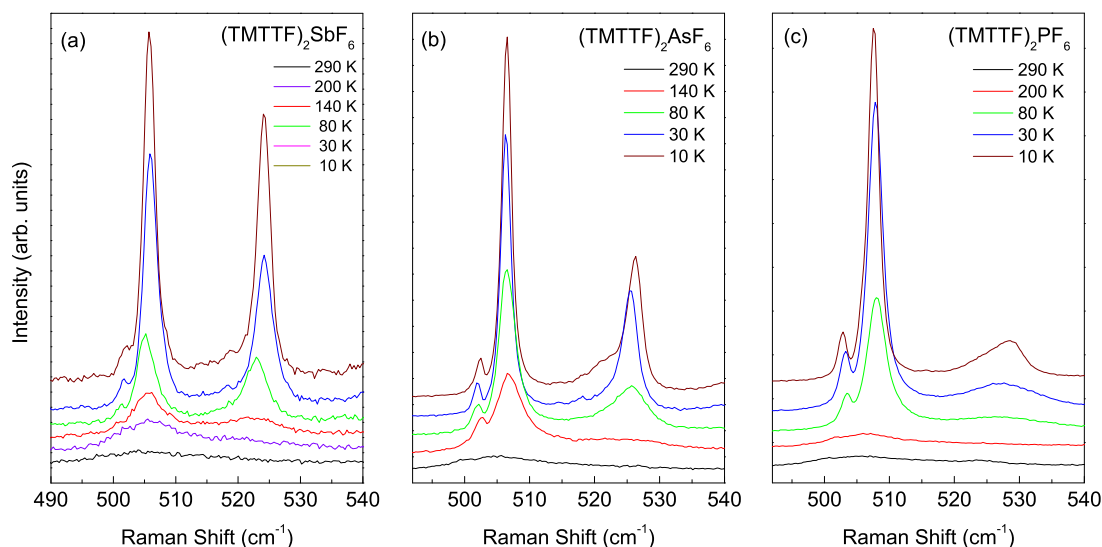


FIG. 4. Temperature dependence of the Raman bands attributed to the ring breathing mode  $\nu_{10}(a_g)$  in the salts  $(\text{TMTTF})_2X$  ( $X = \text{SbF}_6, \text{AsF}_6, \text{PF}_6$ ).

(strong resonance Raman effect). Nevertheless, it is probable that the band at  $1428\text{ cm}^{-1}$ , clearly observed in the spectra of all three salts, could be attributed to the  $\nu_4(a_g)$  mode of the TMTTF<sup>+</sup> ion. Originally, this feature was assigned to Raman active C-H bending vibrations of methyl groups, together with other two bands at  $1446$  and  $1460\text{ cm}^{-1}$  [16] – all these bands are well seen in Figs. 1, 2, and 3. However, on closer examination it appears that the  $1428\text{ cm}^{-1}$  feature is broader than the other two and most probably it consists of several components which could be related to both TMTTF<sup>+</sup> ions and methyl groups. Similarly, the band at  $1578\text{ cm}^{-1}$  may be considered as a superposition of the  $\nu_3(a_g)$  mode of TMTTF<sup>+</sup> ions and the antiphase combination of the  $\nu_{28}(b_{1u})$  mode of (TMTTF)<sub>2</sub><sup>+</sup> dimers.

The observation presented here for the quasi-one-dimensional (TMTTF)<sub>2</sub>X compounds should be compared

with those obtained for quasi-two-dimensional organic systems, such as  $\alpha$ -(BEDT-TTF)<sub>2</sub>I<sub>3</sub>, where charge order also leads to a splitting of the vibrational features in several modes and where domain walls have been suggested based on dielectric spectroscopy [24,25]. Based on this analogy, it might be worth to reconsider the low-frequency dielectric response [7–13] in the different TMTTF salts.

## ACKNOWLEDGMENTS

We thank Marc Fourmigué for high-quality samples and discussions, and Alberto Girlando and Matteo Masino for discussions. We acknowledge support from the German Academic Exchange Service (DAAD).

- 
- [1] F. Nad and P. Monceau, *J. Phys. Soc. Jpn.* **75**, 051005 (2006).
- [2] P. Monceau, J.-L. Lasjaunias, K. Biljaković, and F. Nad, in *The Physics of Organic Superconductors and Conductors*, edited by A. Lebed (Springer, Berlin, 2008), p. 277.
- [3] S. A. Brazovskii, in *The Physics of Organic Superconductors and Conductors*, edited by A. Lebed (Springer, Berlin, 2008), p. 313.
- [4] S. Tomić and M. Dressel, *Rep. Prog. Phys.* **78**, 096501 (2015).
- [5] M. de Souza and J.-P. Pouget, *J. Phys.: Condens. Matter* **25**, 343201 (2013).
- [6] M. Dressel, *Naturwissenschaften* **94**, 527 (2007).
- [7] F. Nad, P. Monceau, C. Carcel, and J. M. Fabre, *Phys. Rev. B* **62**, 1753 (2000).
- [8] F. Nad, P. Monceau, C. Carcel, and J. M. Fabre, *J. Phys.: Condens. Matter* **12**, L435 (2000).
- [9] F. Ya. Nad, P. Monceau, C. Carcel, and J. M. Fabre, *Synth. Met.* **133–134**, 265 (2003).
- [10] P. Monceau, F. Ya. Nad, and S. Brazovskii, *Phys. Rev. Lett.* **86**, 4080 (2001).
- [11] F. Nad, P. Monceau, L. Kaboub, and J. M. Fabre, *Europhys. Lett.* **73**, 567 (2006).
- [12] D. Starešinić, K. Biljaković, P. Lunkenheimer, and A. Loidl, *Solid State. Commun.* **137**, 241 (2006).
- [13] S. Brazovskii, P. Monceau, and F. Ya. Nad, *Physica B* **460**, 79 (2015).
- [14] M. Dressel, M. Dumm, T. Knoblauch, B. Köhler, B. Salameh, and S. Yasin, *Adv. Condens. Matter Phys.* **2012**, 398721 (2012).
- [15] M. Meneghetti, R. Bozio, I. Zanon, C. Pecile, C. Ricotta, and M. Zanetti, *J. Chem. Phys.* **80**, 6210 (1984).
- [16] M. Dressel, M. Dumm, T. Knoblauch, and M. Massino, *Crystals* **2**, 528 (2012).
- [17] M. Dumm, B. Salameh, M. Abaker, L. K. Montgomery, and M. Dressel, *J. Phys. IV France* **114**, 57 (2004).
- [18] M. Dumm, M. Abaker, M. Dressel, and L. K. Montgomery, *J. Low Temp. Phys.* **142**, 613 (2006).
- [19] T. Knoblauch and M. Dressel, *Phys. Status Solidi (C)* **9**, 1158 (2012).
- [20] C. S. Jacobsen, D. B. Tanner, and K. Bechgaard, *Phys. Rev. B* **28**, 7019 (1983).
- [21] D. Pedron, R. Bozio, M. Meneghetti, and C. Pecile, *Phys. Rev. B* **49**, 10893 (1994).
- [22] K. Yamamoto and K. Yakushi, *J. Phys IV France* **114**, 153 (2004).
- [23] A. Frąckowiak and R. Świątlik (unpublished).
- [24] T. Ivek, B. Korin-Hamzić, O. Milat, S. Tomić, C. Clauss, N. Drichko, D. Schweitzer, and M. Dressel, *Phys. Rev. Lett.* **104**, 206406 (2010).
- [25] T. Ivek, B. Korin-Hamzić, O. Milat, S. Tomić, C. Clauss, N. Drichko, D. Schweitzer, and M. Dressel, *Phys. Rev. B* **83**, 165128 (2011).